Applied Energy 97 (2012) 609–617

Contents lists available at SciVerse ScienceDirect

Applied Energy

journal homepage: www.elsevier.com/locate/apenergy

Thermodynamic analysis of two micro CHP systems operating with geothermal and solar energy

Duccio Tempesti *, Giampaolo Manfrida, Daniele Fiaschi

Università degli Studi di Firenze, Dipartimento di Energetica "Sergio Stecco", Via di Santa Marta, 3, 50139 Firenze, Italy

ARTICLE INFO

Article history:
Received 27 July 2011
Received in revised form 6 February 2012
Accepted 8 February 2012
Available online 7 March 2012

Keywords:
Organic Rankine cycles
Combined heat and power
Geothermal energy
Solar energy
Exergy analysis

ABSTRACT

Micro combined heat and power (CHP) plants operating through an organic Rankine cycle (ORC) using renewable energy are analyzed. The reference system is designed to produce 50 kWe. The heat sources of the system are geothermal energy at low temperature (80–100 °C) and solar energy. Two different system layouts, a single and a double stage arrangement, are presented. The first uses a solar field composed only by evacuated solar collectors, and work is produced by a single turbine. In the double-stage system, a field of evacuated solar collectors heats the working fluid up to an intermediate temperature. After this first stage, only a part of the working fluid flow rate is heated in a second solar field, composed of direct-steam parabolic through collectors (PTCs), up to the maximum temperature of the cycle. The mechanical work is then produced in two turbo-expanders arranged in series. For the investigations, different working fluids (e.g. R134a, R236fa, R245fa) are considered. The results of the simulation in terms of efficiencies, heat and electricity production and the main characteristics of the system (i.e. heat exchanger surface, solar collector area) are presented and discussed.

1. Introduction

Organic Rankine power cycles are becoming a leading technology for energy conversion, especially to convert low-temperature heat source. The use of an organic vapour in place of steam is very interesting for small/medium size power plants (50–5000 kW or more, at present). Available heat sources are solar energy [1–3], geothermal energy [4–16], biomass [17–20], and waste heat from various thermal processes (industrial energy intensive process [21,22], gas turbines [23–25], internal combustion engines [26,27]). Geothermal and biomass CHP ORC are already mature technology [28].

Many papers studied ORC system powered by low temperature geothermal resources [5,7,9,10–12]. Since the working fluid determines the optimal resource utilization, and thus the economics of the plant, most of these papers were dedicated to the selection of the proper fluids using very different optimum criteria [5–14,29]. The performances of the geothermal ORC plants were measured in terms of first and second law efficiencies. Energy efficiency is usually in the range 5–15% while exergy efficiency is typically in the range 20–54% [8,15].

Heberle and Brüggemann [5] investigated a second law analysis for the series and parallel circuits of an organic Rankine cycle (ORC) and an additional heat generation for combined heat and power generation. The working fluids investigated were R227ea, R245fa, pentane and isopentane. Results showed that a series circuit with isopentane was most efficient. For parallel circuits and for power generation, R227ea was preferred.

Borsukiewicz-Gozdur and Nowak [7] investigated a method to raise the power of ORC, fuelled by 80–120 °C geothermal water, without an additional input of external energy. This method, however, reduces the cycle efficiency.

Hettiarachchi et al. [9] presented a cost-effective optimum design criterion for Organic Rankine power cycles driven by low-temperature geothermal heat source (70–90 °C) and using HCFC123, *n*-pentane, ammonia or PF5050 as working fluid.

Guo et al. [10] developed a novel cogeneration system that consists of a ORC driven by a low-temperature geothermal resource, an intermediate heat exchanger and a commercial R134a-based heat pump system. The system produces electrical energy by the ORC turbine, while a circuit of heating supply water is fed through the heat released at the ORC condenser, the intermediate heat exchanger and the heat pump. Performances of the CHP system, operating under ideal and disturbance conditions, were compared for eight different working fluids. The geothermal source temperature is in the range 80–100 °C, while the authors supposed to cool the geothermal source down to very low temperature, as 30 °C or even 10 °C. R236ea and R245ca showed the best performances.

Shengjun et al. [11] investigated the parameter optimization and performance comparison of the fluids for subcritical and

* Corresponding author. Tel.: +39 0554796737.
E-mail addresses: duccio.tempesti@unifi.it (D. Tempesti), manfrida@unifi.it (G. Manfrida), daniele.fiaschi@unifi.it (D. Fiaschi).

0306-2619/$ - see front matter © 2012 Elsevier Ltd. All rights reserved.
doi:10.1016/j.apenergy.2012.02.012

Nomenclature

A_{coll}	solar collector area (m^2)
EFF_{sys}	thermal efficiency of the heating system
EI	electrical index
ETH	total space heating energy demand per year (kW h/year)
EXD	exergy destruction (kW)
EXL	exergy loss (kW)
Ex_{cond}	exergy output at condenser (kW)
Ex_{dsh}	exergy output at DSH (kW)
Ex_{geo}	exergy from the geothermal (kW)
Ex_{sun}	exergy from the sun (kW)
G_{tot}	global radiation on the tilted surface
m	mass flow rate (kg/s)
p	pressure (bar)
PEX	yearly primary energy consumption for space heating (kW h/m^2 year)
Q	heat rate (kW)
Q_{cond}	heat recovered at the condenser (kW)
Q_{DSH}	heat recovered at the DSH (kW)
Q_{geo}	geothermal power input (kW)
Q_{solar}	solar radiation incident to collector (kW)
$q_{SH,i}$	space heating demand at the daily hour i (kW)
RP	recirculation coefficient
T	temperature (K)
T_{avcoll}	average temperature of the collector thermal fluid (K)
T_{sun}	temperature of the sun (K)
U	global heat exchange coefficient (kW/m^2-K)
x	quality
W	work (kW)
W_{net}	net power output of the cycle (kW)
W_p	pump power consumption (kW)
W_t	power output of the cycle (kW)
[1]...[n]	thermodynamic point of the cycle
η_{coll}	collector efficiency
η_{system}	system efficiency
η_{cycle}	cycle efficiency

Suffixes

ain	collectors outlet
amb	ambient
aout	collectors inlet
coll	collector
cond	condenser
geoin	geothermal inlet to the system
geoout	geothermal reinjection into the well
geo	geothermal
p	pump
r	relative (referred to overall exergy input)
t	turbine

Acronyms

COND	condenser
DSH	de-super-heater
ECO	economizer
ETC	evacuated solar collectors
EVA	evaporator
GEO HX	geothermal heater
HPP	high pressure pump
HPT	high pressure turbine
LPP	low pressure pump
LPT	low pressure turbine
PTC	parabolic trough collectors
RHE	regenerative heat exchanger
SH	super-heater

transcritical ORC powered by a geothermal source at 90 °C. They used five indicators – thermal efficiency, exergy efficiency, recovery efficiency, heat exchanger area per unit power output (APR) and the levelized energy cost (LEC) – for the evaluation and the comparison. They found that the optimum operation parameters are not the same for different indicators.

Saleh et al. [12] investigated 31 different pure working fluids suitable for ORC system fuelled by a low-temperature geothermal resource (100 °C or somewhat higher). They considered different cycles in base of the shape of the T-s diagram of the working fluid. These cycles were compared in terms of thermal efficiency, volume flow rate at turbine inlet and expansion ratio. Desideri and Bidini [13] compared in terms of efficiency and power generation three configurations of ORC fuelled by geothermal sources (150–210 °C) with conventional single and dual flash power plants. A regenerated ORC with a closed heat exchanger was the solution recommended for liquid-dominated geothermal sources. Lakew and Bolland [29] compared power production capability of a simple subcritical ORC driven by low-temperature (80–200 °C) heat source with different working fluids (R134a, R123, R227ea, R245fa, R290, and *n*-pentane). R227ea gives highest power for heat source temperature range of 80–160 °C and R245fa produces the highest in the range of 160–200 °C.

Bruhn [14] examined a geothermal fossil hybrid technology for steam power plants (500 MWel). He proposed to replace the conventional preheating process, where feedwater for the boiler is preheated by steam extracted from the turbine, with preheating with a geothermal resource at low temperature. Thus, the extraction steam which remains in the turbine leads to an increased power output. This process could contribute either to an increase in the power output (booster operation) or to combustible fuel saving at a constant power output (fuel-saver operation). Bruhn found that if water at sufficient temperature is available close to steam power plants at moderate depths, a project of geothermal preheating can be successful both economically and ecologically without any subsidy.

Borsukiewicz-Gozdur [15] proposed hybrid power plant to increase the utilization of geothermal resource supposed available at 80–120 °C, i.e. to reduce the temperature of the returned geothermal water. The author proposed two solutions, a dual-fluid hybrid power plant and an hybrid power plant. The proposed dual-fluid power plant consists of an upper Hirn cycle, in which water is vapourized in a biomass boiler and is then condensed in a condenser–vapourizer exchanger, which is the thermal link between the upper and lower cycles. The lower cycle is an ORC where the organic liquid is preheated by the geothermal resource. Thus, in this dual-fluid power plant, the low-pressure part of the classical steam–water power plant (i.e. condenser) is replaced by a ORC.

As in [14], the geothermal water could also be used for preheating of the working fluid (water or another substance) in a single cycle power plant. Borsukiewicz-Gozdur [15] called this cycle simply hybrid plant, and chose a biomass boiler for the upper part of the cycle, while the working fluid selected is cyclohexane. In the calculation, Borsukiewicz-Gozdur [15] supposed to reject the geothermal water down to a very low temperature, i.e. 35 °C. The author found out that, with the scope to use the least share of energy from other sources than geothermal, the best option would be a dual-fluid-hybrid power plant with R236fa as a working fluid for the ORC cycle. However, a rejection temperature of 35 °C seems very low and could be achieve only with a geothermal resource without any salt, i.e. only water.

At Cerro Prieto, Mexico, geothermal wells supply directly the geothermal steam at different temperature (200–150 °C) to an open Rankine cycle for electricity generation. When the wells provide a mixture of liquid and steam, steam is separated from liquid by a separator (single flash power plant), and the remaining liquid is sent either to a second separation system (double flash) or to an evaporation pond. Lentz and Almanza [6] proposed to add a parabolic trough solar field to increase the steam flow at the existing geothermal cycle. Two alternatives were investigated: the first with the solar field between the wells and the first separator, the second with the solar field between the first and the second separator. This configuration will increase the capacity factor of the system by generating additional steam during the peak demand hours. However, the increase in flow is limited by the content of dissolved salts.

Astolfi et al. [16] proposed to integrate a concentrating solar power system into a supercritical ORC, designed for the optimal utilization of an intermediate enthalpy geothermal source (150 °C). After the primary heat exchanger between the working fluid (R134a) and the geothermal resource, high temperature heat source derived from solar parabolic trough field heat up R134a, increasing electricity production. The authors stated that the integration with a solar field could improve the attractiveness of the many low-enthalpy geothermal sources that are widespread around the world.

Considering only ORC system fuelled by low-temperature geothermal resources, more attention has been given to the selection of the appropriate working fluid for the given operating data. Few Refs. [5,10] investigated CHP ORC system powered by low-temperature geothermal resource. All the few works on the geothermal hybrid systems [6,14–16] investigated only power plant for electricity production (at least 1 MWel, up to 550 Mwel). Also, in three cases the geothermal resource is at medium temperature [6,14,16], and in one case the geothermal resource is considered as a booster in a fossil fuel power plant [14]. Only [15] considered a power plant for electricity production fuelled by geothermal at low-temperature and another renewable energy resource, i.e. biomass. Any reference that investigated a CHP ORC system powered by low-temperature geothermal resource and another renewable energy was found in literature.

In this paper, two innovative CHP ORC systems powered by low-temperature geothermal resource (i.e. 90 °C) and solar energy captured by solar collectors are described. The systems proposed have a small size (i.e. 50 kWel) because, differently from the system proposed since now in the literature [6,14–16], they are thought for small CHP applications, as for instance for buildings of 30–40 apartments. The performances of both systems in design condition using three suitable working fluids are discussed. Also, for the most promising combination of system and fluid in terms of heat available for cogeneration, a preliminary analysis of the performance of the system during the heating season is presented. Finally, future steps of the work are presented.

2. Thermodynamic conditions

The reference case here considered has a high-end (turbine inlet) temperature of 420 K. This choice reflects interest for applications of low- and medium-enthalpy geothermal resources, or solar thermal power plants using solar collectors without concentrators (such as evacuated glass heat pipe solar collectors), or with a limited concentration ratio (thus, having a low cost of installation and more limited optical off-axis performance deterioration, with respect to large solar thermal power plants). The idea is developing small power units (50 kW is the reference size here considered), discharging heat at temperature in the range of 60–80 °C, that is appealing for domestic heating (in winter), or even for air conditioning (in summer, coupled with an absorption cycle refrigeration unit). The electrical efficiency of the cycle is expected to be low (7–11%), but electricity should be seen as a by-product with respect to the main issue, the heat recovered for domestic heating, hot water production or cooling system.

3. Power plant layout – single-pressure, dual circuit

Fig. 1 represents the single-pressure cycle configuration of the power plant. The micro-turbine expander inlet is typically in slightly superheated conditions; the regenerator at discharge can be required or not depending on the shape of the T-s diagram

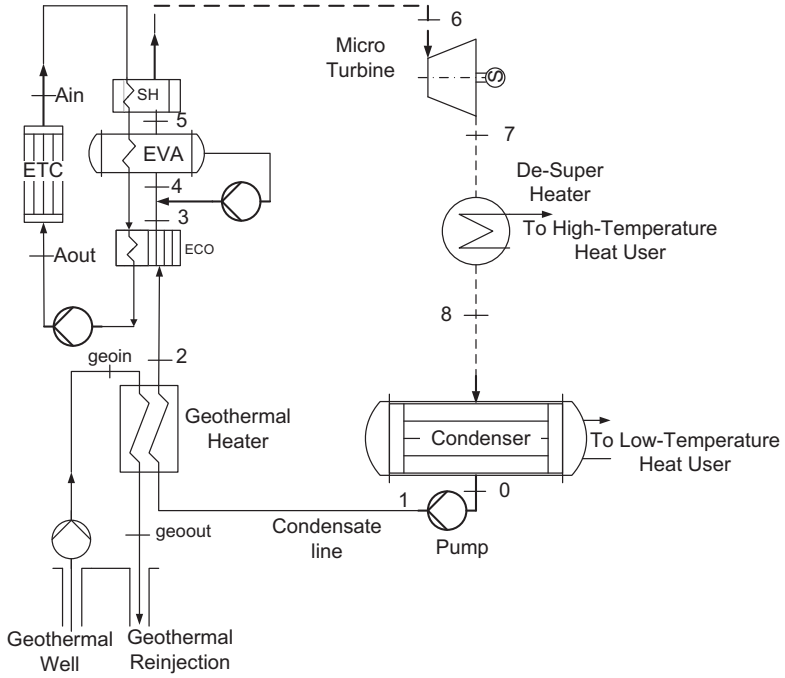

Fig. 1. Single-pressure geothermal/solar ORC layout.

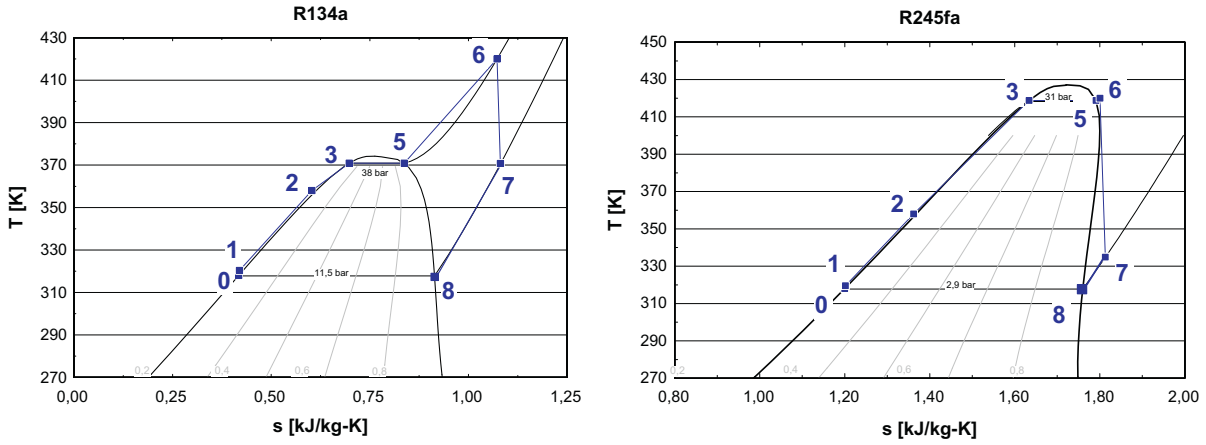

Fig. 2. Thermodynamic cycles for R134a (left) and R245fa (right).

(it is recommended if the end of expansion lies in highly superheated conditions, see Fig. 2).

The different shape of the cycle in the T-s diagram is shown in Fig. 2, referring to fluids R134a (left) and R245fa (right).

The liquid organic fluid coming from the condenser is first preheated in a heat exchanger (geothermal heater, Fig. 1) by a geothermal flow rate at low temperature (363 K). Then, the organic fluid is heated up to the maximum temperature – set at 420 K – passing through a heat exchanger connected to an Evacuated Tube Collectors (ETCs) field. This corresponds to current state of the art of SEGS, using a high-temperature heat transfer fluid in the solar collectors. After producing mechanical work in the turbine, the organic fluid has still high temperature and enthalpy values. This heat is recovered in building heating and domestic hot water production (CHP unit). From the point of view of combined heat and power, it is important to separate the de-super-heater DSH (providing heat at higher temperature, but with limited heat capacity) from the condenser (providing heat at low and constant temperature, but with infinite heat capacity). The organic fluid at turbine outlet is then first cooled from superheated conditions down to saturated vapour conditions at variable temperature (DSH). The DSH can be connected to a domestic heating system operating at medium–low temperature (typically, 333–313 K), which can be used for domestic hot water or for a heating system at medium temperature. Then, the saturated organic vapour is condensed at constant temperature, producing low-temperature hot water at 313 K, exploitable in a domestic heating system at low temperature. The organic fluid is then circulated to the geothermal heater by the pump to start the cycle again (point [1], Fig. 1).

Data on air temperature, global and direct radiation for a town located in central Italy were acquired from a long-term local data source [30]. The design conditions for the CHP plant were taken in terms of air temperature, global and direct radiation at 13:00 of a reconstructed standard day in March. Calculations were carried out by a model developed through Engineering Equation Solver (EES® [31]). In order to simplify safety problems in a CHP unit for residential applications, engineered refrigerants suitable for low-temperature energy conversion were selected: R134a, R236, R245fa [12,32]. EES® provides built-in thermophysical property data for these fluids. Table 1 reports the parameters used for the calculations. The collector is modelled by a quadratic approximation [33]:

$$\eta_{coll} = c_0 - \left[(c_1 + c_2 \cdot (T_{avcoll} - T_{amb})) \cdot \left(\frac{T_{avcoll} - T_{amb}}{G_{tot}}\right)\right] \quad (1)$$

where T_{avcoll} is the average temperature of the collector thermal fluid and T_{amb} is the air temperature. For the evacuated solar collector, the operating data for an ESTEC VR12 CPC® were used [33]. The temperature difference between the collector thermal fluid at collector outlet and the maximum temperature of the organic fluid is set at 10 K. The temperature difference between the geothermal fluid and the organic fluid at geothermal heat exchanger outlet (point [2]) is set at 5 K. The refrigerant fluid enters the condenser at 310 K, which is the return temperature from the building heating system.

3.1. Performance evaluation (single pressure)

Application of the model allows to calculate the main performance indicators. The system efficiency is calculated by:

$$\eta_{system} = \frac{W_{net}}{Q_{geo} + Q_{solar}} \quad (2)$$

Table 1
Parameters used for the calculations.

Cycle		Solar	
Turbine power output W_t (kW)	50	Tilt angle (°)	30
Condenser temperature T_0 (K)	318	Optical efficiency c_0	82.5
Maximum cycle temperature T_6 (K)	420	Coefficient c_1 (W/(m^2 K))	0.91
Pump isentropic efficiency	0.8	Coefficient c_2 (W/(m^2 K^2))	0.6×10^{-3}
Turbine isentropic efficiency	0.8	T_{ain}–T_6 (K)	10
		Pinch point temperature difference (K)	5
ECO – U (kW/(m^2 K))	0.25	Global irradiation on the 30° tilted surface G_{tot} (W/m^2)	931
EVA – U (kW/(m^2 K))	0.20		
SH – U (kW/(m^2 K))	0125	Ambient temperature (K)	284
Geothermal		Condenser	
Geothermal temperature (T_{geoin}) (K)	363	Refrigerant inlet temperature (K)	310
Geothermal heat exchanger U (kW/(m^2 K))	0.30	Temperature difference pinch point (K)	5
Temperature difference T_{geoin}–T_3 (K)	5	DSH U (kW/(m^2 K))	0.125

where W_{net} is the net power output of the cycle, Q_{geo} is the thermal power supplied by the geothermal resource and Q_{solar} is the solar radiation incident on to the collector. Q_{solar} is calculated by the product of the collector total area and the global radiation on the tilted surface (30°), G_{tot}.

The cycle efficiency is defined as:

$$\eta_{cycle} = \frac{W_{net}}{Q_{geo} + Q_{coll}} \quad (3)$$

where Q_{coll} is the power captured by the collector, i.e. the product of Q_{solar} and of the collector efficiency η_{coll} (Eq. (1)). The flow rate m_{solar} of the heat transfer fluid circulating in the primary collector loop is calculated through the enthalpy balance at the evaporator and the super-heater (EVA + SH), while the solar collector area A_{coll} is calculated using the collector energy balance:

$$m_{solar} \cdot (h_6 - h_3) = G_{tot} \cdot \eta_{coll} \cdot A_{coll} \quad (4)$$

Heat exchanger surfaces are calculated through the NTU-effectiveness method [34], assuming the values of the overall heat transfer coefficient U listed in Table 1 for each heat exchanger section. The results obtained for the value of $p[1]$ (upper cycle pressure) that maximizes the cycle efficiency are reported in Table 2.

The highest cycle efficiency is obtained with R245fa. Using R245fa leads to the lowest values of the working fluid flow rate (1.33 kg/s), solar collectors area (305 m^2), and pump power demand (3.6 kW). However, the lowest quantity of heat is recovered at the condenser in the R245fa cycle, especially at the DSH where only 23 kW at 330 K are recovered. This result is due to the low value of the working fluid flow rate and to the low temperature at the turbine outlet (335 K). For cogeneration purpose, R134a seems to be the more interesting fluid, because it allows to recover nearly 400 kW at DSH and condenser. In particular, it could heat 0.45 kg/s of water up to 367 K, allowing to use it also for a high temperature heating system. The cycle efficiency (9%) is the lowest of the three cases, but this is not important for this power plant, because the thermal input is obtained from renewable resources. The Electric Index is also common for evaluating the cogeneration performances of the system:

$$EI = \frac{W_{net}}{Q_{cond} + Q_{DSH}} \quad (5)$$

The R245fa cycle achieves the highest value of electrical index (Table 2). In addition, R245fa requires the lowest geothermal flow rate, in this case m_{geo} = 0.49 kg/s. R236fa gives intermediate results between the other two fluids, except for the highest organic flow rate (1.84 kg/s). In all three cases, the geothermal resource supplies approximately 25% of the thermal energy required by the cycle.

Table 2
Calculations results for the single pressure layout.

Fluid	R134a	R236fa	R245fa
Critical pressure (bar)	40.59	32	36.5
Critical temperature (K)	374	398	427
Upper cycle pressure $p[1]$ (bar)	38	29.3	31
Condenser pressure $p[0]$ (bar)	11.6	5	2.92
Geothermal reinjection temperature (K)	321	323	323
$T[6]$–$T[5]$ (K)	49	26	1.3
Temperature at DSH inlet $T[8]$ (K)	371	366	335
Water temperature at DSH outlet (K)	367	359.5	330
Organic fluid flow rate (kg/s)	1.77	1.84	1.33
Turbine exhaust volume flow rate (m^3/s)	0041	0067	0088
Geothermal flow rate (kg/s)	0.63	0.59	0.43
Solar collector flow rate (kg/s)	1.1	1.16	3.45
Collector unit surface flow rate (l/(hm^2))	10.29	12.53	44.25
Water flow rate at DSH (kg/s)	0.45	0.43	0.32
Water flow rate at condenser (kg/s)	22.3	19.72	18.93
Collectors effective area (m^2)	411	356	305
System efficiency (%)	9.1	9.78	13
Cycle efficiency (%)	10.5	11.3	15.1
Exergy efficiency (%)	22.7	23.3	25.0
Geothermal power input Q_{geo} (kW)	111	98.5	72.4
Solar power input Q_{solar} (kW)	316	273.5	235
DSH heat recovered (kW)	102	82.5	23
Condenser heat recovered (kW)	280	247	237.5
Pump power W_p (kW)	5.1	7.8	3.6
$Q_{geo}/(Q_{geo} + Q_{solar})$ (%)	26	26.5	23.6
$W_p/(W_p + W_t)$ (%)	10.3	16	7.3
Geothermal heat exchanger surface (m^2)	535	183.5	69
ECO surface (m^2)	35.5	29.6	14.2
EVA surface (m^2)	37.4	32.4	58
SH surface (m^2)	40.6	34.2	4
DSH surface (m^2)	224	100.6	37.6
EI	0.12	0.13	0.18

3.2. Exergy analysis (single pressure)

An exergy analysis of the single pressure power plant has been performed, in order to assess the exergy destruction within components and the exergy losses from the system.

The calculation approach to exergy balance of power cycle follows the reference literature [35,36]. The exergy inputs to the system come from (I) geothermal and (II) sun. The exergy from the sun is given by:

$$EX_{sun} = G_{tot} \cdot A_{coll} \cdot \left[1 - \frac{T_{amb}}{T_{sun}}\right] \quad (6)$$

where T_{sun} is taken as 75% of the equivalent black-body sun temperature, in agreement with [3,37]. Hence, the exergetic efficiency is defined as follows:

$$\eta_{ex} = \frac{W_{net} + Ex_{dsh} + Ex_{cond}}{Ex_{sun} + Ex_{geo}} \quad (7)$$

where Ex_{sun} has been previously explicated, while W_{net} is the net power output of the cycle. Furthermore, Ex_{geo} is the exergy from the geothermal resource, while Ex_{dsh} and Ex_{cond} are the exergy outputs of the heat transferred for cogeneration uses at DSH and COND. As for the cycle efficiency, the highest exergetic efficiency is obtained with the R245fa.

The relative exergy destructions (EXD_r) and losses (EXL_r) of power plant components (scaled to the overall exergy input) are shown in Fig. 3. The highest value of exergy destruction (approximately 50%) comes from the collector. This result is due to the degradation of the heat from the sun temperature (5800 K) down to

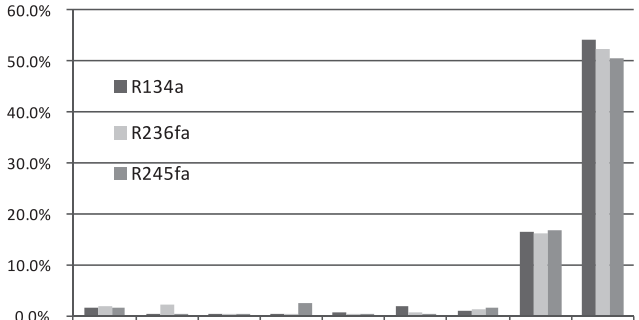

	DSH+ COND	Pump	Geo HX	ECO	EVA	SH	Turbine	ETC EXL	ETC EXD
R134a	1.6%	0.2%	0.1%	0.1%	0.7%	1.8%	1.1%	16.5%	54.1%
R236fa	1.7%	2.1%	0.2%	0.1%	0.3%	0.6%	1.3%	16.2%	52.4%
R245fa	1.7%	0.2%	0.2%	2.5%	0.4%	0.0%	1.7%	16.7%	50.6%

Fig. 3. Relative exergy destructions and losses of plant components (single pressure).

the collector temperature (350 K or less). Also, since the collector temperature is greater than the ambient temperature, the exergy loss from the collector to the ambient is relevant (16.5%). It is important to notice that the EXD_r in the DSH + COND is very low because these components release heat to cogeneration uses, and not to the ambient as in a traditional power plant (see Eq. (7)).

4. Power plant layout – dual pressure, single circuit

The second configuration of the power plant is built around a dual-pressure system, using two different solar collectors (Fig. 4).

The system takes full advantage of modern direct vapour-producing collectors, which are currently under development for steam [38]. This allows to apply a scheme using a single circuit for the heat transfer fluid in the solar collectors, and for expansion in the ORC turbine. The organic fluid is first directly heated by the ETC and then by the Parabolic Trough Collectors (PTCs) fields. The ETCs are used only for liquid preheating (ETC-1) and phase transition (ETC-2), with a recirculation loop producing vapour of limited quality (typically $x[5] = 10\%$) for optimization of heat transfer performance. A vessel is used for separating the saturated vapour phase, part of which ($m[7]$) is directed to the low-pressure turbine (LPT). An appropriate amount $m[6]$ of the saturated liquid phase in the separation vessel is compressed and directed to the high-pressure loop using PTCs, were the working fluid is produced in superheated conditions at exit. In practice, once $x[5]$ is given, $m[15]$ is obtained by the flow rate balance at the vessel, and the ratio $m[6]/m[5]$ is a design variable controlling the relative size of the ETC and PTC solar collector fields. In operative off-design conditions with variable radiation, the recirculation flow rate $m[15]$ can be used to control the value of $x[5]$. This new layout allows to increase the maximum temperature, because PTCs have a better efficiency and can reach higher temperatures than ETC.

Table 3
Additional parameters needed for the dual pressure system.

Cycle		PTC	
HP pump efficiency	0.8	Optical efficiency c_0 PTC	69.3
HPT efficiency	0.8	C_1 PTC (W/(m^2 K))	0.48
LPT efficiency	0.8	C_2 PTC (W/(m^2 K^2))	0.3×10^{-3}
Fluid quality ETC outlet	0.1		
Collectors flow rate ratio m_5/m_6	3	Direct radiation (W/m^2)	730

The following Table 3 summarizes the values of the additional parameters needed for the dual-pressure system. The PTC efficiency is calculated by Eq. (1) using different parameters, and the operating data of IST® were used [33].

4.1. Performance evaluation (dual pressure)

The system and the cycle efficiencies are still calculated by Eqs. (2) and (3), respectively, considering the layout modifications (two collectors fields – ETC and PTC –, global radiation for ETC and direct radiation for PTC). Table 4 reports the results of the calculations. Here again, the upper pressure of the cycle $p[8]$ was set at a value maximizing the cycle efficiency. The calculations showed that the constraints on the geothermal resource (temperature and flow rate) influence this second layout more than the single pressure layout. In the R134a cycle, only by setting the intermediate pressure $p[1]$ at 32 bar it is possible to reach good cycle efficiency values, because at lower $p[1]$ values, the geothermal contribution is small.

Furthermore, the ETC flow rate is very high: 215 l/(hm^2) for the R245fa, and up to 388 l/(hm^2) for the R134a. Since the organic fluid flow rate circulating in the power plant is higher than in the previous case, the hot water flow rate heated by the DSH and the

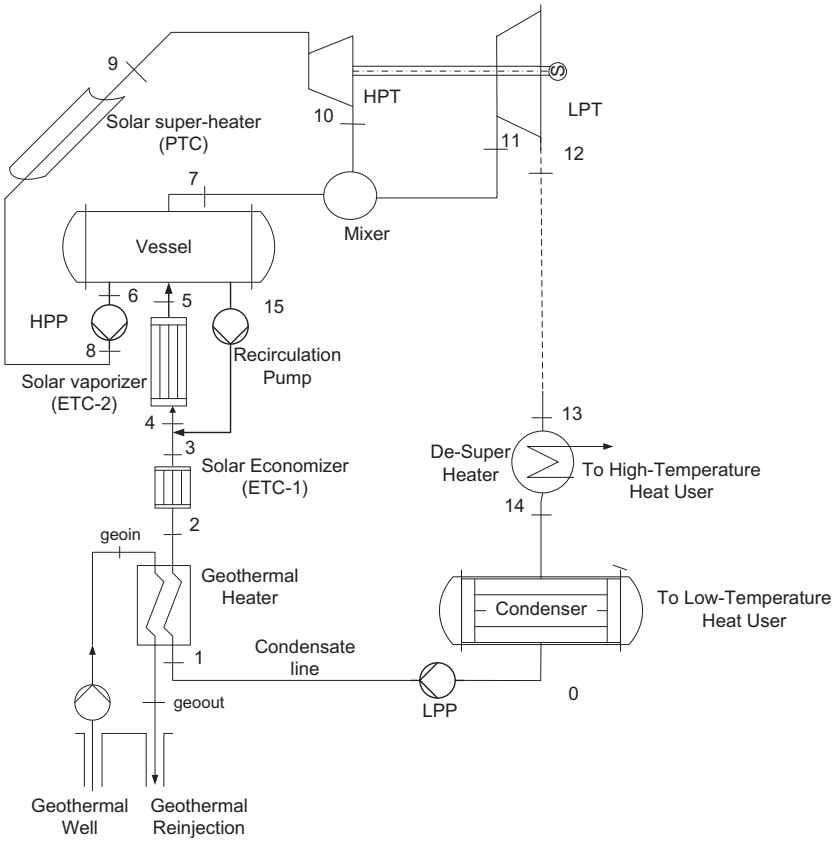

Fig. 4. Dual-pressure geothermal/solar ORC layout.

Table 4
Calculations results for the dual pressure layout.

Fluid	R134a	R236fa	R245fa
Maximum pressure (bar)	38	29.3	31
Condenser pressure (bar)	11.6	5	2.92
Intermediate pressure p_1 (bar)	32	16	16
Geothermal reinjection temperature (K)	335	330	330
Temperature at DSH inlet T_{12} (K)	358.2	360.4	338.6
Water temperature at DSH outlet (K)	350.5	356.6	333.5
ETC flow rate m_5 (kg/s)	5.07	5.28	3.65
Recirculation flowrate (kg/s)	2.87	2.99	2.07
HPT flowrate m_{10} (kg/s)	1.69	1.78	1.21
LPT flowrate m_{12} (kg/s)	2.19	2.29	1.58
HPT volume flow rate (m^3/s)	0.01	0019	0013
LPT volume flow rate (m^3/s)	0.04	0081	0106
PTC unit surface flowrate (l/(hm^2))	12.8	12.5	12.8
ETC unit surface flowrate (l/(hm^2))	388	272.8	215.1
ETC eco unit surf. flowrate (l/(hm^2))	141.1	145.7	48.8
Geothermal flow rate (kg/s)	1.02	0.79	0.55
Water flow rate at DSH (kg/s)	0.62	0.49	0.39
Water flow rate at condenser (kg/s)	27.6	24.5	22.4
Total collector area (m^2)	665.3	592	479.5
ETC eco area (m^2)	59.2	49.7	99.1
ETC area (m^2)	55.6	64.8	58.4
PTC area (m^2)	490	477	322
System efficiency (%)	6.9	7.4	10.0
Cycle efficiency (%)	8.9	9.5	12.7
Exergetic efficiency (%)	17.5	18.4	20.0
Geothermal power input Q_{geo} (kW)	120.1	109.3	76.6
Solar power input Q_{solar} (kW)	366.6	329.4	283.8
DSH heat recovered (kW)	96.7	90	33.2
Condenser heat recovered (kW)	443.2	397	314.5
Pump power (kW)	6.4	8.3	4.2
$Q_{geo}/(Q_{geo} + Q_{solar})$ (%)	24.7	24.9	21.3
$W_p/(W_p + W_t)$ (%)	12.9	16.5	8.3
EI	9.8	10.5	14.6

condenser is increased, the same happens for the total collector surface. Another effect of the increase of the organic fluid flow rate is the augmentation of the power input to the cycle, i.e. the sum of the solar power collected by ETC and PTC fields and power coming from geothermal resource. For this reason, cycle and system efficiencies are lower than in the single pressure layout.

4.2. Exergy analysis (dual pressure)

Also for the dual pressure power plant an exergy analysis has been carried out. Eqs. (6)–(8) have been used, replacing the total radiation with the direct radiation.

The relative exergy destructions (EXD_r) and losses (EXL_r) of power plant components (scaled to the overall exergy input) are shown in Fig. 5. The highest value of exergy destruction comes from the PTC, where approximately the 30–40% of the exergy input is destroyed. Also the first relevant exergy loss takes place in the PTC (from 15% to 25%). R245fa leads to either a relevant EXD in the ECO ETC field or a decrease of the EXD and EXL of the PTC section. In all the three cases, the exergetic efficiency is lower than in the single pressure power plant (Table 4).

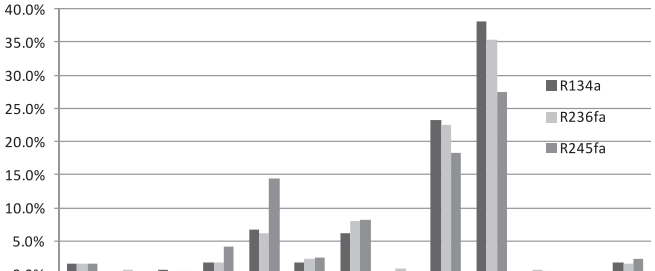

	DSH+ COND	LPP	GEO HX	Etc-1 EXL	Etc-1 EXD	Etc-2 EXL	Etc-2 EXD	HPP	PTC EXL	PTC EXD	HPT	Mixer	LPT
R134a	1.6%	0.2%	0.7%	1.8%	6.7%	1.7%	6.2%	0.0%	23.2%	38.1%	0.2%	0.3%	1.8%
R236fa	1.5%	0.6%	0.3%	1.7%	6.1%	2.2%	8.0%	0.9%	22.5%	35.4%	0.5%	0.1%	1.6%
R245fa	1.5%	0.1%	0.5%	4.1%	14.5%	2.4%	8.2%	0.1%	18.3%	27.5%	0.5%	0.0%	2.3%

Fig. 5. Relative exergy destructions and losses of plant components (dual pressure).

5. Preliminary analysis – CHP performance

The previous analysis showed that the single pressure dual circuit layout operating with R134a is the most promising system in terms of heat generation. Thus, a preliminary analysis of the performance of the system during the heating season has been carried out. A thorough analysis of this aspect is not the purpose of this work, and will be the subject of future work, investigating also the design of the heating system and the use of heat for air conditioning. In a domestic CHP system, the user's thermal demand is a main issue, particularly the distribution during each day and each month of the heating season. Since the hot water demand is a small fraction of the space heating, the thermal load curve is here assumed to be given also by the space heating. The space heating load curve is influenced by many factors, as the ambient air temperature or the season. Fig. 6 presents the dimensionless space heating hourly demand ($q_{SH;i}$) for a residential user in two standard days of December and of January (the month with the peak thermal demand). These normalized profiles were built taking into account the monthly variation of ambient temperature in the heating season for the city considered (1 November – 31 March) [39]. The normalized profiles of Fig. 6 can be used to calculate the hourly thermal energy load for space heating [40]. First of all, it is important to estimate the total thermal energy demand per year (E_{TH}) for space heating of a residential household. The yearly primary energy consumption for space heating (PEC_{SH}) depends on various factors, as the weather data, the building design (especially, the ratio between the heated surface (S) and corresponding volume (V)), and the thermal properties (mainly the conductivity and thermal resistance) of the envelope of the building. In this preliminary analysis, PEC_{SH} has been fixed at 100 kW h/year per m^2 of heated surface, while the heated surface (S) has been fixed at 70 m^2 and the total number of heated apartments (n_{apts}) has been fixed at 30. E_{TH} and the hourly average power (kW h/h) for space heating ($Q_{TH;SH}$) are calculated using the following equations:

$$E_{TH} = PEC_{SH} \cdot S \cdot EFF_{sys} \cdot \eta_{apts} \tag{8}$$

$$E_{TH} = Q_{TH;SH} \cdot \sum_{i=1}^{3648} (q_{sh;i}) \tag{9}$$

where EFF_{sys} is thermal efficiency of the heating system (i.e. distribution and regulation of the heating system), fixed at 0.96.

The hourly space heating demand profile is then obtained multiplying $Q_{TH,SH}$ by the hourly normalized thermal demand (Fig. 6). In Fig. 7, the continuous line represents the hourly space heating demand, while the dashed curve shows the thermal energy generated by the system in a standard day of December and January. The thermal energy generated by the system exceeds the thermal energy demand only during the sunny hours of the day (10–17). Thus, thermal energy storage must be inserted in the system so that the thermal energy in excess can be used during the hours when the system cannot satisfy the thermal energy demand. At the end of the day, the energy balance between the thermal energy produced by the system and the thermal energy load will lead to a surplus or a gap of thermal energy (Table 5). In all the months except December, there is a thermal energy surplus. In this case, thermal energy storage must be designed in order to collect this surplus of thermal energy. In December, instead, there is a gap in the thermal energy

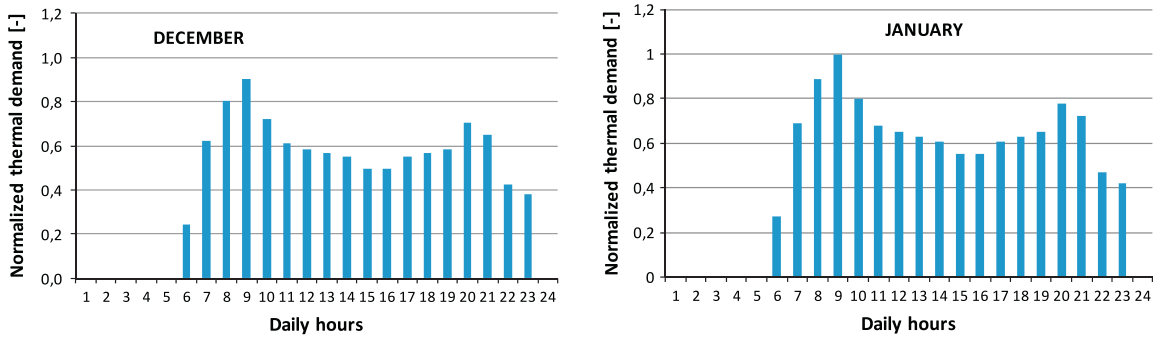

Fig. 6. Normalized space heating hourly demand for December (left) and January (right).

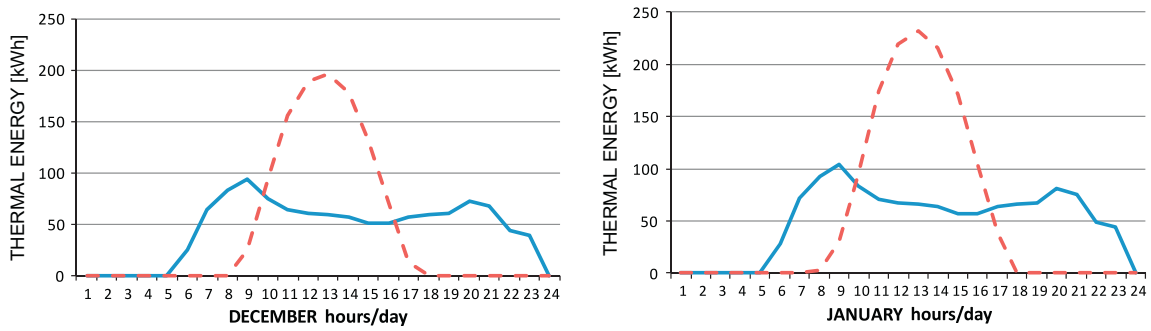

Fig. 7. Hourly space heating demand (continuous) and hourly thermal energy generated by the system (dashed) for a standard day of December and January.

Table 5
Thermal energy Gap (minus) or Surplus (plus) for a standard day.

	Thermal energy gap/surplus
November	218 kW h
December	−154 kW h
January	75 kW h
February	789 kW h
March	1847 kW h

balance, which means that the thermal energy needs of the building must be supplied in a different way (for instance, using directly the geothermal energy resource to feed the heating system). In this way, the system would not produce electrical energy, which however, could be easily taken from the electricity grid.

6. Conclusions

In this paper, two CHP ORC schemes powered by low-temperature geothermal resource (i.e. 90 °C) and solar energy captured by solar collectors have been presented. The system proposed has a small size (50 kWel, 400 kWt), which makes it appropriate for small CHP applications (i.e. buildings with 30–40 apartments). The performance of both configurations (single-pressure with heat transfer fluid; and dual-pressure with direct-steam collectors) has been calculated comparing three different fluids: R134a, R236fa, R245fa. In both configurations, the best performances were obtained with R245fa in terms of cycle and exergy efficiency; with R134a in terms of heat recovered at the DSH and condenser. For the single-pressure layout operating with R134a, a preliminary analysis of the performance of the system during the heating season has been carried out. It was found that the system can satisfy the space heating demand for 30 apartments during all the heating season, except for December. Furthermore, the results showed that with reference to design conditions, for this low-temperature application, the traditional single pressure layout with double circuit has a better performance than the dual-pressure solution. The minor plant complexity is another aspect that makes the single pressure configuration more attractive than the dual pressure option. In principle, the dual-pressure solution is, however, more flexible and can be more adaptable to working in off-design conditions, which shall be subject of further research.

Acknowledgements

This research has been funded by Regione Toscana, project "BT-GEO H&P: – Sistemi di Generazione Distribuita di Energia Elettrica e Termica da Fonti Geotermiche", using European Social Fund (FSE) resources.

References

[1] Schuster A, Karellas S, Kakaras E, Spliethoff H. Energetic and economic investigation of organic Rankine cycle applications. Appl Therm Eng 2009;29:1809–17.
[2] Zhai H, Dai YJ, Wu JY, Wang RZ. Energy and exergy analyses on a novel hybrid solar heating, cooling and power generation system for remote areas. Appl Energy 2009;86:1395–404.
[3] Fiaschi D, Lifshitz A, Manfrida G. Fuel-assisted solar thermal power plant with supercritical ORC cycle. In: Proceedings of ECOS2010, Lausanne; 2010.
[4] Di Pippo R. Geothermal power plants: Principles, applications and case studies. London, UK: Elsevier Advanced Technology; 2006.
[5] Heberle F, Brüggemann D. Exergy based fluid selection for a geothermal organic Rankine cycle for combined heat and power generation. Appl Therm Eng 2006;30:1326–32.
[6] Lentz A, Almanza R. Solar–geothermal hybrid system. Appl Therm Eng 2006;26:1537–44.
[7] Borsukiewicz-Gozdur A, Nowak W. Comparative analysis of natural and synthetic refrigerants in application to low temperature Clausius–Rankine cycle. Energy 2007;32:344–52.
[8] Franco A, Villani M. Optimal design of binary cycle power plants for water-dominated, medium-temperature geothermal fields. Geothermics 2009;38:379–91.
[9] Hettiarachchi HD, Golubovic M, Worek WM, Ikegami Y. Optimum design criteria for an organic Rankine cycle using low-temperature geothermal heat sources. Energy 2007;32:1698–706.

[10] Guo T, Wang HX, Zhang SJ. Selection of working fluids for a novel low-temperature geothermally-powered ORC based cogeneration system. Energy Convers Manage 2011;52:2384–91.
[11] Shengjun Z, Huaixin W, Tao G. Performance comparison and parametric optimization of subcritical Organic Rankine cycle (ORC) and transcritical power cycle system for low-temperature geothermal power generation. Appl Energy 2011;88:2740–54.
[12] Saleh B, Koglbauer G, Wendland M, Fjscher J. Working fluids for low-temperature organic Rankine cycles. Energy 2007;32:1210–21.
[13] Desideri U, Bidini G. Study of possible optimization criteria for geothermal power plants. Energy Convers Manage 1997;38:1681–91.
[14] Bruhn M. Hybrid geothermal–fossil electricity generation from low enthalpy geothermal resources: geothermal feed water preheating in conventional power plants. Energy 2002;27:329–46.
[15] Borsukiewicz-Gozdur A. Dual-fluid-hybrid power plant co-powered by low-temperature geothermal water. Geothermics 2010;39:170–6.
[16] Astolfi M, Xodo L, Romano MC, Macchi E. Technical and economical analysis of a solar–geothermal hybrid plant based on an organic Rankine cycle. Geothermics 2011;40:58–68.
[17] Turboden combined heat and power orc units for the pellet industries, (see also <http://www.turboden.eu/en/public/press/Turboden_ORC_for_pellets_english.pdf>); 2008.
[18] Dong L, Liu H, Riffat S. Development of small-scale and micro-scale biomass-fuelled CHP systems – a literature review. Appl Therm Eng 2009;29:2119–26.
[19] Drescher U, Bruggemann D. Fluid selection for the organic Rankine cycle (ORC) in biomass power and heat plants. Appl Therm Eng 2007;27:223–8.
[20] Obernberger I, Hammerschmid A, Biomass fired CHP plant based on an ORC cycle – project ORC-STIA-Admont. Final report. Bios-energy systems; 2001.
[21] Bonilla JJ, Blanco JM, Lσpez L, Sala JM. Technological recovery potential of waste heat in the industry of the Basque country. Appl Therm Eng 1997;17:283–8.
[22] BCS Inc. Waste heat recovery: technologies and opportunities in US industry, US Dept of Energy (DOE); 2008.
[23] Invernizzi C, Iora P, Silva P. Bottoming micro-Rankine cycles for micro-gas turbines. Appl Therm Eng 2007;27:100–10.
[24] Chacartegui R, Sánchez D, Muñoz JM, Sánchez T. Alternative ORC bottoming cycles for combined cycle power plants. Appl Energy 2009;86:2162–70.
[25] Al-Sulaiman FA, Dincer I, Hamdullahpur F. Exergy analysis of an integrated solid oxide fuel cell and organic Rankine cycle for cooling, heating and power production. J Power Sources 2010;195:2346–54.
[26] Vaja I, Gambarotta A. Internal Combustion Engine (ICE) bottoming with Organic Rankine cycles (ORCs). Energy 2010;35:1084–93.
[27] GE energy announces industrial waste-heat recovery innovation for onsite power plants; 6 July, 2009 [accessed 04.01.12].
[28] Tchanche BF, Lambrinos Gr, Frangoudakis A, Papadakis G. Low-grade heat conversion into power using organic Rankine cycles – a review of various applications. Renew Sust Energy Rev 2011;15:3963–79. <http://www.genewscenter.com/content/detail.aspx?releaseid=7229&newsareaid=2>.
[29] Lakew AA, Bolland O. Working fluids for low-temperature heat source. Appl Therm Eng 2010;30:1262–8.
[30] Agency for environmental protection of Tuscany. Meteorological measured data internal report, 1991–2004, Florence; 2005.
[31] Klein SA. Engineering equation solver. Academic Version V8.603.
[32] ElectraTherm's Heat to Power Generation Systems, <http://www.electratherm.com/products.html> [accessed 04.01.12].
[33] Aiguasol Enginyeria. Poship final report: the potential of solar heat for industrial processes project no. NNE5-1999-0308. European Commission Directorate General Energy and, Transport; 2001.
[34] Nellis GF, Klein SA. Heat transfer. Cambridge (UK): Cambridge University Press; 2009 [www.fchart.com].
[35] Bejan A. Entropy generation through heat and fluid flow. John Wiley & Sons Inc.; 1982.
[36] Kotas TJ. The exergy method of thermal plant analysis, London. Boston: Butterworths; 1985.
[37] Farahat S, Sarhaddi F, Ajam H. Exergetic optimization of flat plate solar collector. Renewable Energy 2009;34:1169–74.
[38] Eck M, Zarza E. Saturated steam process with direct steam generating parabolic troughs. Sol Energy 2006;80:1424–33.
[39] Bianchi M, Ferrari C, Melino F, Peretto A. Feasibility study of a thermo – photo – voltaic system for CHP application in residential buildings. In: Proceedings of third international conference on applied energy, Perugia (Italy); 2011.
[40] Bianchi M, De Pascale A, Spina P. Best practice in residential micro-CHP systems design. In: Proceedings of third international conference on applied energy, Perugia (Italy); 2011.